17B.2 **HI-RES GRIDDED MOS 6-H QPF GUIDANCE**

Jerome P. Charba*
Frederick G. Samplatsky
Meteorological Development Laboratory
Office of Science and Technology
National Weather Service
Silver Spring, Maryland

1. INTRODUCTION

The gridded National Digital Forecast Database (NDFD; Glahn and Ruth 2003) has recently become the flagship product (NWS 2007) in the National Weather Service (NWS). The corresponding National Digital Guidance Database (NDGD) has also been implemented to support and supplement NDFD. One of the weather elements in the current suite of NDGD suite of gridded products is 6-h quantitative precipitation forecasts (QPF), which is produced by applying a special objective analysis program to model output statistics (MOS; Glahn and Lowry 1972) 6-h QPFs issued at irregularly spaced stations (Glahn et al. 2009).

In this paper, the focus is also on the production of gridded, statistically-based 6-h QPF guidance, but here the QPFs are specified directly on a fine mesh grid rather than indirectly through post-processing of station oriented forecasts. This direct approach, along with new types of gridded ingested data, accommodates incorporating enhanced spatial and intensity resolution into the QPFs. In this article, key features of the new gridded MOS QPF model are summarized, its forecast skill is examined, and plans for its operational implementation are noted.

2. PROPERTIES OF QPF MODEL

As with the station oriented 6-h QPF product, the new model is based on the MOS technique (Glahn and Lowry 1972). But, it contains key extensions, which include a fine mesh (4-km) native grid framework, inclusion of fine scale topography and precipitation climatologies, and geographical regionalization. These extensions accommodate the incorporation of fine spatial detail in the QPF products, especially in areas of steep mountain slopes of the western United States (U.S.). The new techniques also support enhanced precipitation intensity resolution in the QPF products.

The MOS technique uses multiple linear regression equations to produce estimates (forecasts) of the predictand. Here the predictand was defined from gridded radar-based 6-h precipitation estimates in the eastern U.S. and a special climatology-enhanced objective analysis of gage precipitation observations in the West, both of which are known as the "Stage III" precipitation analysis [Charba and Samplatsky 2009a (hereafter cited as CS) and references therein]. The Stage III analyses are produced regionally for subsets of a 4-km nationwide grid at each of the 12 NWS River Forecast Centers over the contiguous U.S. (CONUS). The regional grids are composited at the central computing facility of the NWS National Centers for Environmental Prediction (NCEP) to form the (national) Stage IV precipitation analysis (http://www.emc.ncep.noaa.gov/mmb/ylin/pcpanl/stage4/). The latter grids were quality controlled at the NWS Meteorological Development Laboratory prior to application here.

The QPF predictands for a 4-km grid box were defined as (eight) cumulative categories of 6-h precipitation that range ≥ 0.01 inch to ≥ 2.00 inch. The predictors, which were specified at the centers of the grid boxes, were derived from the NCEP Global Forecast System (GFS; Iredell and Caplan 1997) model output together with fine scale precipitation climatologies and topography. The regression equations yield probabilities for each of the eight precipitation categories (PQPFs). In addition, three precipitation variables are derived from the PQPFs, which consist of the probability weighted amount (same as expected value), "best category", and a continuous amount. These four QPF products are (presently) issued twice daily from the 0000 and 1200 UTC cycles for 6-h projections in the 12 – 120 h range over the CONUS (Fig. 1). All

* *Corresponding author address:*
Dr. Jerome P. Charba, National Weather Service
1325 East West Highway, Room 10410
Silver Spring, MD 20910-3283
email: jerome.charba@noaa.gov

QPF products will be made available on the CONUS NDFD grid.

The regression equations were developed from archived data for the period January 2001 to March 2007 and tested on an April 2007 - March 2008 independent sample. Separate equations were developed for the 0000 and 1200 UTC cycles and for the warm (April – September) and cool (October – March) seasons. A signature feature of the equations is their geographical stratification. Specifically, separate equations were derived for each of the 13 regions shown in Fig. 1. Initially, we used the discrete regions in this figure, which were formed through a simple partitioning of the CONUS domain. (A discussion of the rational basis of these regions is contained in CS.)

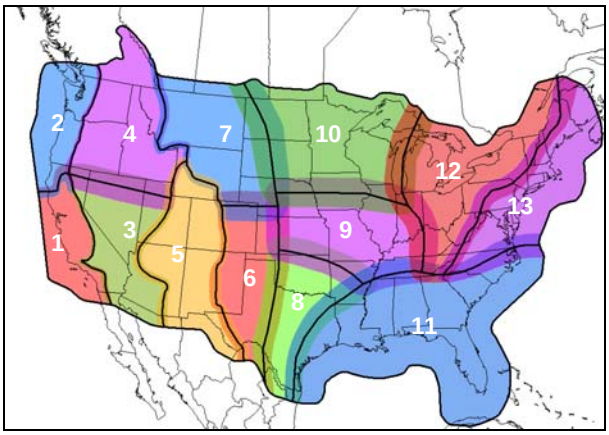

Figure 1. Geographical coverage (multi-color shading), which is partitioned into 13 discrete regions (bounded by bold black lines and numbered 1 to 13) and corresponding overlapping regions (color shading). The color shades change where neighboring regions overlap.

The application of these discrete region equations revealed a significant problem, however, which was that non-meteorological discontinuities in the probability fields appeared along region boundaries. An example in Fig. 2a shows artificial perturbations along region boundaries (Fig 1) in Arkansas, Illinois, Indiana, Pennsylvania, and Tennessee. The discontinuities result from inter-regional variations in the regression equations, which result from many factors including regional variations in precipitation mechanisms, systematic error in predictor variables, and predictand climatology.

The discontinuity problem was addressed by expanding the discrete regions such that neighboring regions overlap one another (Fig. 1). Note that the degree of overlap along the discrete region boundaries varied substantially among the 13 regions. For "natural" region boundaries (most common to regions 1 - 7), where spatial gradients in precipitation climatology and terrain elevation are strong (CS), the overlap is small. Conversely, the overlap is much larger for quasi-arbitrary boundaries, where the corresponding spatial gradients are weak. Details concerning the boundary overlap are also contained in CS.

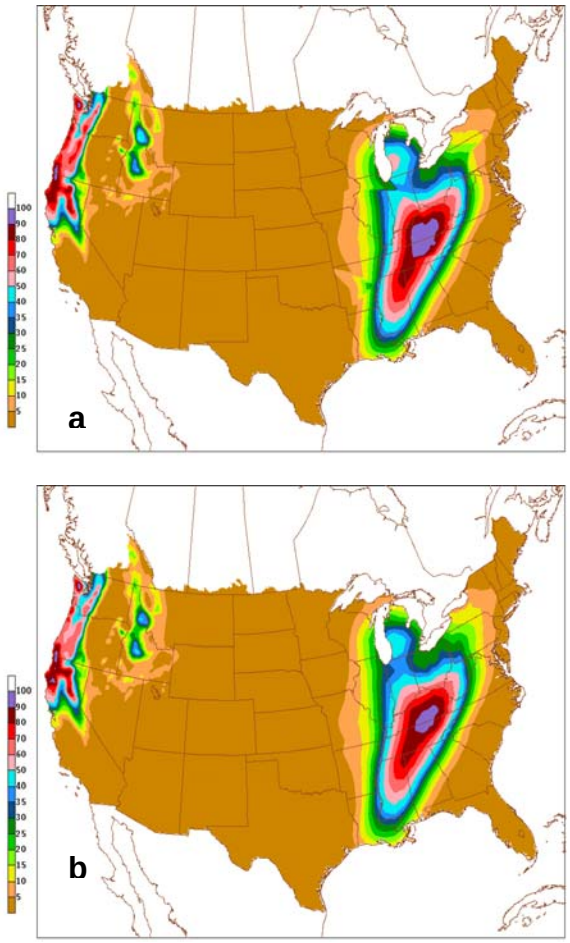

Figure 2. Smoothed 36-h forecast probability (%) of ≥ 0.10 inch for the 6-h period ending 0000 UTC 30 January 2008 produced with (a) the discrete regions and (b) overlapping regions approaches.

The PQPF regression equations were then developed for the overlapping regions, which (ulti-

mately) results in multiple PQPFs for grid points in the overlap zones (CS). For these points, single PQPFs are obtained as a weighted sum of the multiple values, where the sum of the weights is 1.0.

The weight(s) at any grid point (non-overlapping or overlapping) consist of pre-determined constants. For a non-overlap point the weight is inherently 1.0. For an overlap point the computed weights are inversely related to the distances of the point to the associated (overlap) region boundaries. The weights computation formula ensures that the sum of the individual weights is 1.0 (CS).

For the case in Fig. 2a, the PQPF field with the overlapping regions regression equations and probability weighting procedure is shown in Fig. 2b. Note that the probability pattern with this new approach is very similar to that with the discrete regions, except the non-meteorological perturbations have been effectively "erased." This finding was repeated in many cases examined, which spanned all precipitation thresholds, forecast projections, and both seasons. Also, an important result documented in CS is that verification scores with the new procedure were at least as good as those with the discrete regions.

3. CASE EXAMINATIONS

In this section, the attributes of the 6-h QPFs are examined for three heavy rain cases selected from the independent sample, two of which were from the 2007-08 cool season and the third from the 2008 warm season. The purpose is to illustrate properties of the forecasts and link these to underlying model attributes.

For brevity, just two of the four QPF variables produced by the model are shown here. One is the 6-h PQPFs, as directly produced by the regression equations (Fig. 2). The other variable is a continuous 6-h precipitation amount, which is derived from the PQPFs through a multi-step procedure. [Briefly, the steps to compute a continuous precipitation amount at a grid point include the following. (1) An objectively pre-determined (constant) threshold probability, which is specific to each precipitation category, region, and forecast projection, is applied to the corresponding PQPF value. This results in a set of binary switches that indicate which categories met/did not meet their threshold. (2) A decision tree, comprised of an empirically-determined set of rules, is applied to the set of switches to determine the heaviest precipitation category expected to occur. Note that the precipitation categories have upper and lower precipitation amount bounds, except the highest category (≥ 2.00 inch), which does not have an upper bound. (3) A prescribed algebraic formula is applied to the categorical value (a separate extrapolation formula is applied for the highest category) to obtain a continuous "interpolated" precipitation amount. For the cool (warm) season the maximum continuous 6-h precipitation amount obtained through this process is 4.6 (4.7) inches.]

As a cool season case for the mountainous western U.S., Fig. 3 shows the observed and 12-h/84-h forecast precipitation for the 6-h period ending 0000 UTC 05 January 2008. (Throughout this paper, the valid time of the observed and forecast precipitation is referenced to the end of the 6-h period.) Noteworthy features are: (i) the observed and forecast precipitation patterns, where peak values exceeded 2.50 inch, match remarkably well for both the 12-h (short) and 84-h (long) forecast projections, (ii) the PQPF patterns for the ≥ 0.50 inch threshold at 12 hours (Fig. 3d) and the ≥ 1.00 inch threshold at 84 hours (Fig. 3e) are quite similar to the corresponding forecast precipitation amount patterns (Figs. 3b and 3c, respectively), (iii) the PQPFs for ≥ 0.50 inch are much higher than those for those for ≥ 1.00 inch, and (iv) high values in both the observed and forecast precipitation patterns are aligned along the windward slopes of the Coastal, Sierra Nevada/Cascade Mountain ranges from California to Washington and the Bitter Root range in Idaho (mountain ranges not shown).

Concerning item iii (above), the higher PQPF values for ≥ 0.50 inch compared to those for ≥ 1.00 inch are due to two factors. One is the shorter forecast projection (and thus higher forecast certainty) and the other is the higher climatic relative frequency of occurrence of the ≥ 0.50 inch events.

Regarding item iv (above) the influence of the steep windward and lee slopes of the noted mountain ranges in controlling the fine spatial detail in the distribution of the forecast (and observed) precipitation is especially noteworthy. In fact, the orographic influence is also largely responsible for

the similarity of the fine spatial forecast patterns at the long and short projections. This detail stems from predictor input from the fine scale precipitation climatology and topography. The topo-climatic inputs also introduce fine detail around the Great Lakes and mountainous areas of the eastern U.S. (not shown), but the degree of the control on the precipitation distribution there is less than in the West.

It is noted that three types of fine scale precipitation climatologies were used as predictor input, as the spatial and temporal (time of the day and day of the year) resolution varied substantially among them. Also, because the topo-climatic predictor variables are "present weather ignorant", it was necessary to "interact" them with selected GFS forecast variables. The interactive technique effectively injects the fine topo-climatic detail into

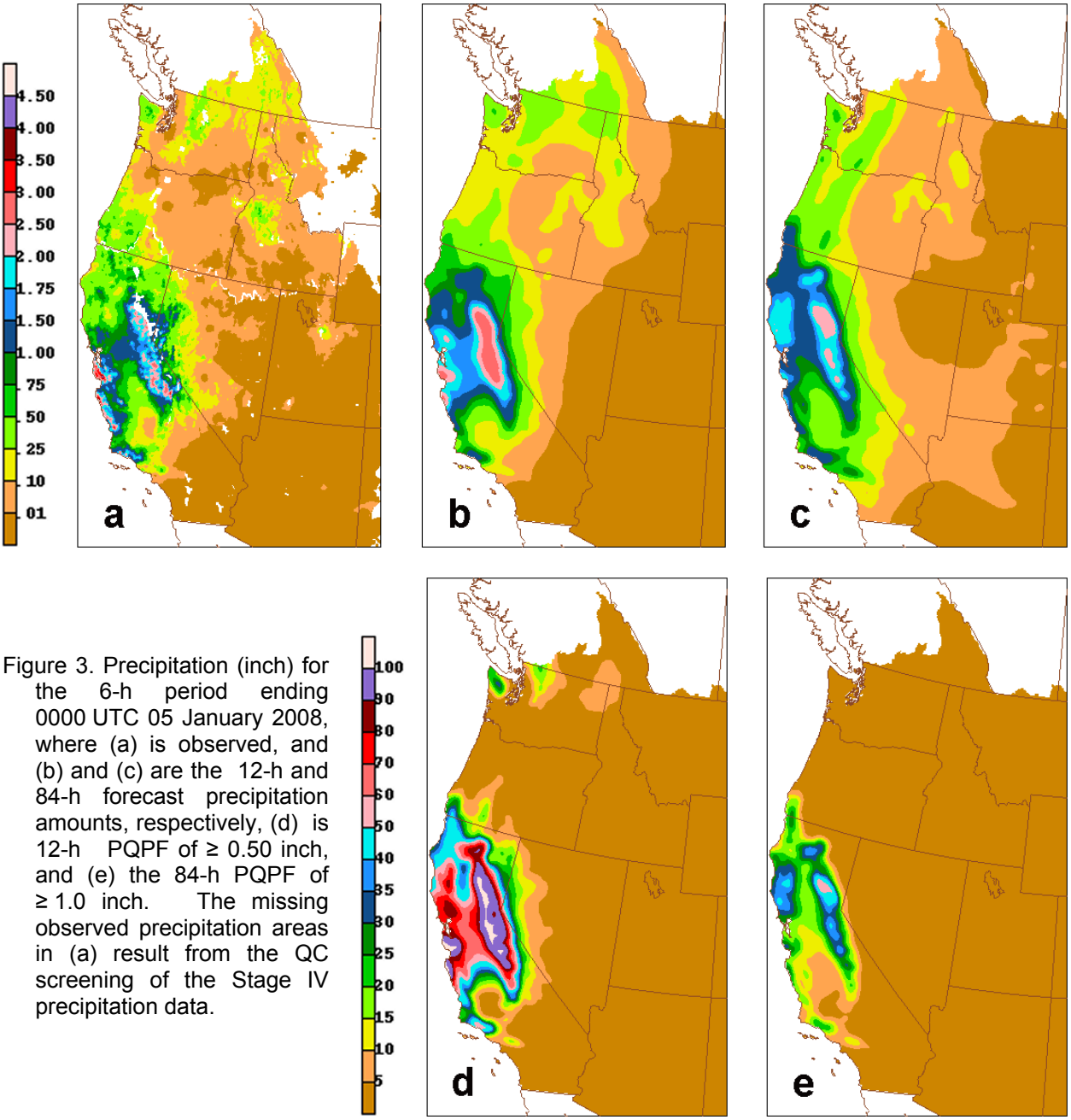

Figure 3. Precipitation (inch) for the 6-h period ending 0000 UTC 05 January 2008, where (a) is observed, and (b) and (c) are the 12-h and 84-h forecast precipitation amounts, respectively, (d) is 12-h PQPF of ≥ 0.50 inch, and (e) the 84-h PQPF of ≥ 1.0 inch. The missing observed precipitation areas in (a) result from the QC screening of the Stage IV precipitation data.

the GFS variables (and ultimately into the QPF products). Details of the topo-climatic data inputs and the interactive technique are both discussed in Charba and Samplatsky (2009b).

Another selected cool season heavy rain event occurred over the central U.S. for the 6-h period ending 0600 UTC 19 March 2008 (Fig. 4). In this case, precipitation in excess of 1.0 inch occurred in a broad band from northeast Texas to Ohio, where isolated amounts above 3.0 inches occurred in Arkansas and southern Missouri (Fig. 4a). Figure 4b shows that the 24-h precipitation amount forecast was very precise, with a peak amounts over 3.5 inches in central Arkansas. Even at 42 hours (Fig. 4c) the forecast amounts in this location were quite accurate, where peak values were over 3.0 inches. As with the previous case, the PQPF patterns for both the ≥ 0.50 inch threshold at the 18-h projection (Fig. 4d) and the ≥ 1.00 inch threshold at the 42-h projection (Fig. 4e) are quite similar to the corresponding precipitation amount forecasts. Also, the lower PQPF values for the latter precipitation threshold and forecast projection (Fig. 4e) are due more to the rarer ≥ 1.00 inch precipitation event than to the longer forecast projection (not shown).

The final case is for the 6-h period ending at 1200 UTC 13 September 2008, when Hurricane Ike caused extensive destruction in Galveston, Texas and nearby areas. Figure 5a shows that observed 6-h precipitation amounts exceeded 2.0 inches over a broad area from the upper Texas coast to the western Louisiana coast, with peak amounts in excess of 4.5 inches. At the same time, extra-tropical heavy rains with peak amounts almost this high occurred in a narrow band from northern Missouri to northwestern Indiana. Figures 5b and 5c show that the extremely heavy rainfall along the Texas - Louisiana coastline was quite accurately predicted for both 24 and 72 hours in

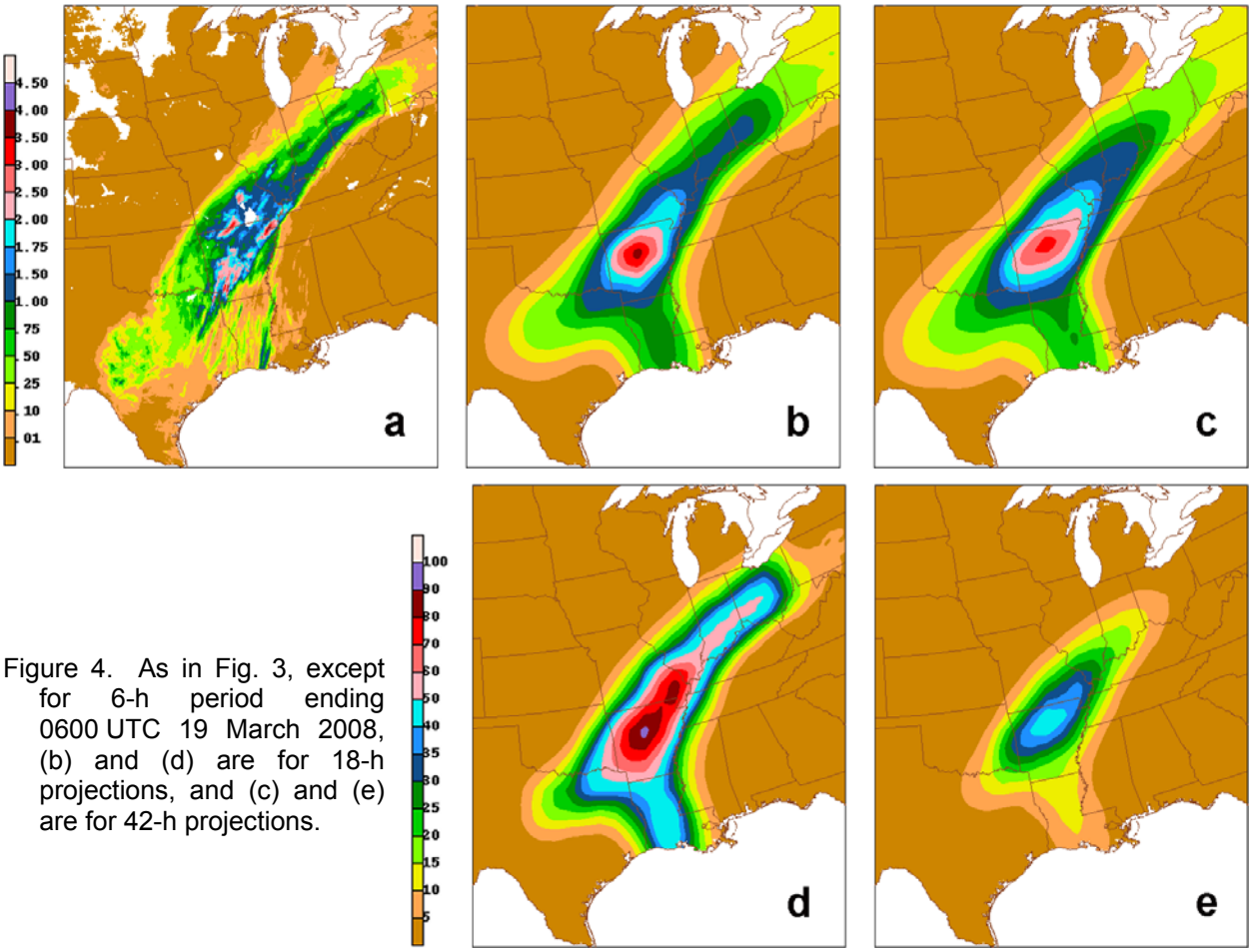

Figure 4. As in Fig. 3, except for 6-h period ending 0600 UTC 19 March 2008, (b) and (d) are for 18-h projections, and (c) and (e) are for 42-h projections.

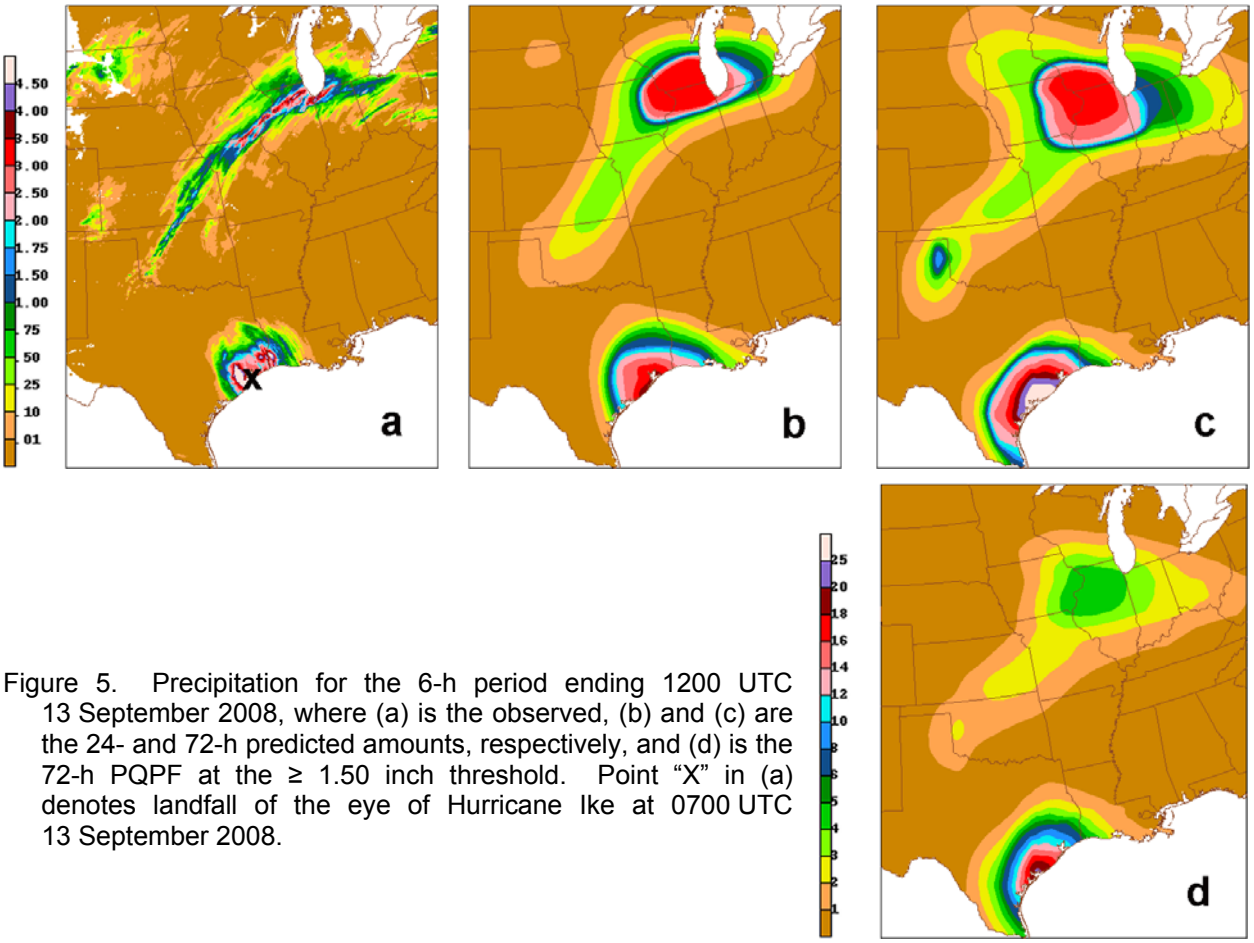

Figure 5. Precipitation for the 6-h period ending 1200 UTC 13 September 2008, where (a) is the observed, (b) and (c) are the 24- and 72-h predicted amounts, respectively, and (d) is the 72-h PQPF at the ≥ 1.50 inch threshold. Point "X" in (a) denotes landfall of the eye of Hurricane Ike at 0700 UTC 13 September 2008.

advance, with minor amount under-forecasting at the shorter projection and a slight (westward) positioning error at the longer projection.

The heavy rains over the upper Midwest were also well predicted, although the predicted patterns were not as narrow as the observed pattern, and peak amounts were slightly under-predicted. On the other hand, a small, peculiar peak above 1.50 inches in the predicted precipitation amount field at the 72-h projection appeared in the eastern Texas Panhandle (Fig. 5c), which did not verify. Note that the PQPF field for the 1.50-inch threshold, which is shown in Fig. 5d, shows only small evidence of a peak in this location. Also, note that the precipitation amount peak appears in the overlap zone for regions 6 and 8 (Fig. 1). Thus, the small erroneous peak arose as a result of an inter-region limitation in the post-processing procedure used to obtain the derived continuous precipitation amount field. Still, examination of a large number of cases of the precipitation amount forecasts has revealed that the appearance of such a procedural artifact is rare.

4. CATEGORICAL SCORES FOR COMPARATIVE QPF PRODUCTS

We conducted comparative performance scoring for a number of operational 6-h QPF products together with the high resolution gridded MOS (HRMOS) QPF products discussed in this paper. The comparative scoring, which was for the 0000 and 1200 UTC cycles and the full October 2007-March 2008 cool season (an independent sample for HRMOS), included 6-h QPFs from the GFS, gridded MOS, HRMOS, NCEP Hydrometeorological Prediction Center (HPC), and NDFD. To date, the scoring is considered preliminary because the QPFs from HRMOS were from an obsolete version of the model, and the NDFD QPFs (included in the scoring) were issued with just a short (2 hour) ad-

vance availability of the most recent HPC QPF guidance. For these reasons and for brevity, only scores from the GFS, HRMOS and HPC QPF guidance are discussed here.

The QPFs included in the scoring were in categorical form, as obtained by converting the continuous analogues into non-occurrence/occurrence categories based on the ≥ 0.01, ≥ 0.10, ≥ 0.25, ≥ 0.50, ≥ 1.00, and ≥ 2.00 inch thresholds. The comparative scoring was conducted by matching the issuance time of each QPF product with the 0000 or 1200 UTC model cycle; the issuance time for the GFS is about 4 hours afterward, HRMOS about 5 hours afterward, and HPC about 12 hours afterward. With this progression of issuance times, the most recent GFS QPF is available for ingest into the HRMOS model, and the GFS and HRMOS QPF guidance products are both available to HPC forecasters.

For brevity, the scores for the individual 6-h projections are combined into 24-h "day" projections, where the 12-, 18-, 24-, and 30-h projections comprise Day 1, the 36-, 42-, 48-, and 54-h projections comprise Day 2, and similarly for Day 3. Figure 6 contains the threat score (same as critical success index, Schaefer 1990) for Day 1 and Day 3 and the bias for Day 2 (which was representative for all three "days"). The charts show that the HRMOS threat scores were slightly better than those for HPC for most precipitation thresholds at the Day 1 projection, and that they were clearly better at all thresholds for Day 3. [For Day 2, the HRMOS improvement on HPC fell between that for Day 1 and Day 3 (not shown).] The GFS threat scores were inferior to both HRMOS and HPC for both Day 1 and Day 3. Regarding the bias (where perfect bias is 1.0), the figure shows that HRMOS was superior to both HPC and the GFS. Both the GFS and HPC tended to over-forecast light precipitation and under-forecast heavy precipitation, where this tendency was especially severe for the GFS. It is noted that the current (upgraded) version of the HRMOS model exhibits a near-constant bias of 1.1 – 1.2 for all thresholds and all projections to 120 hours (not shown).

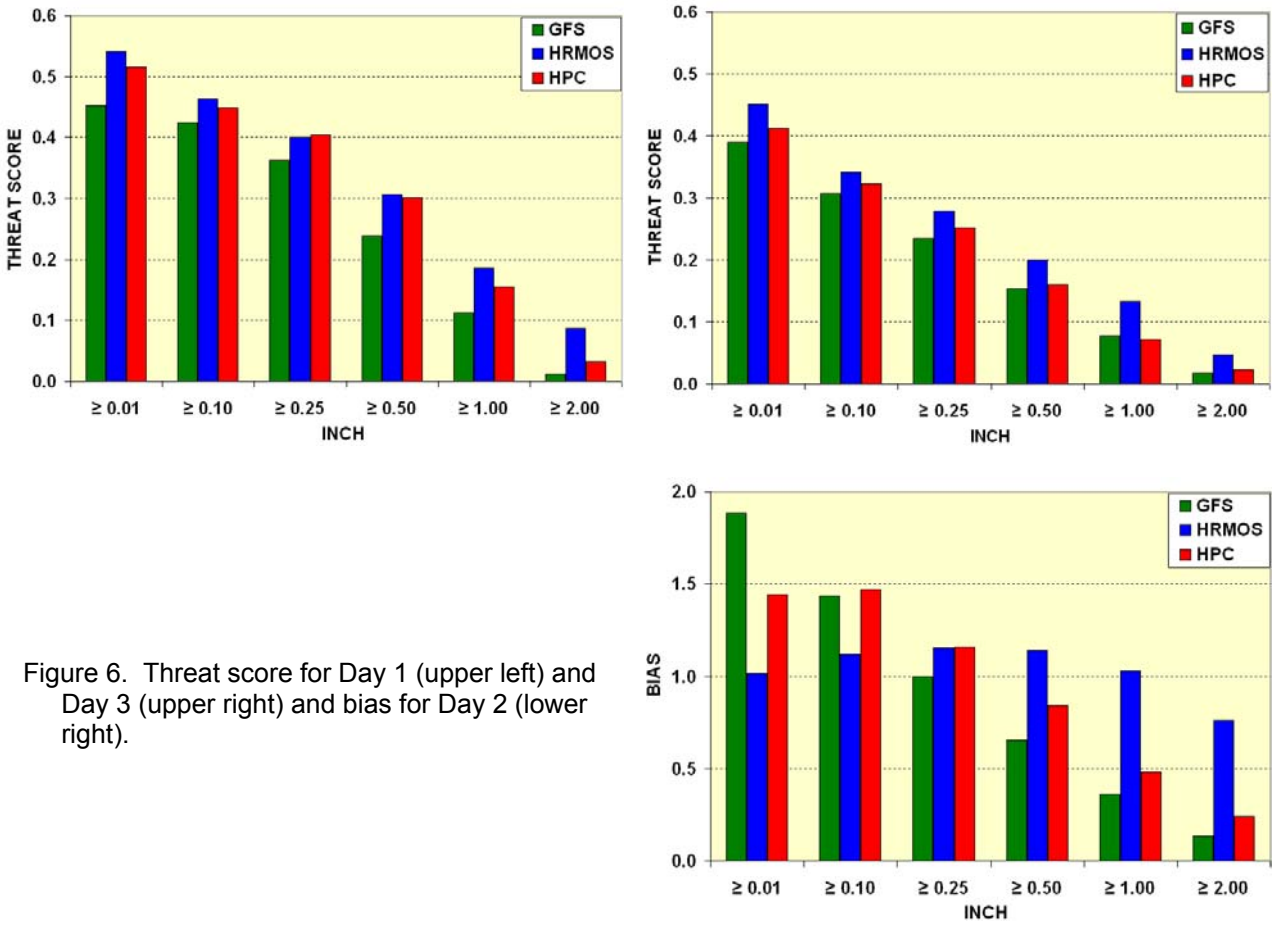

Figure 6. Threat score for Day 1 (upper left) and Day 3 (upper right) and bias for Day 2 (lower right).

5. CURRENT STATUS AND IMPLEMENTATION PLANS

We began running the HRMOS QPF model in a real time test mode for the 0000 and 1200 UTC cycles in June 2008. For the purpose of user feedback, real time QPF graphics have been made available internally within the NWS through a private website and on the AWIPS system (http://www.nws.noaa.gov/ops2/ops24/awips.htm).

Because of the subsequent positive user response to the HRMOS QPF products, in April 2009 we began making preparations for the model's operational implementation. We expect to upgrade the run mode of the model from test to experimental in August 2009, at which time the (still unofficial) products will become available to the public. Finally, we expect the HRMOS QPF guidance will officially replace and supplement the currently operational gridded MOS QPF guidance over the CONUS, which should happen around January 2010.

6. ACKNOWLEDGEMENTS

Letitia Soulliard of the NCEP National Precipitation Verification Unit provided archives of the Stage IV precipitation analyses and the operational HPC and NDFD 6-h QPFs.

7. REFERENCES

Charba, J. P., and F. Samplatsky, 2009a: Regionalization in fine grid quantitative precipitation forecasts. (Conditionally accepted for publication in *Mon. Wea. Rev.*).

____, 2009b: GFS-based MOS 6-h quantitative precipitation forecasts on a 4-km grid. (Manuscript in preparation).

Glahn, H. R., and D. A. Lowry, 1972: The use of Model Output Statistics (MOS) in objective weather forecasting. *J. Appl. Meteor.*, **11**, 1203-1211.

____, B., and D. Ruth, 2003: The new digital forecast database of the National Weather Service. *Bull. Amer. Meteor. Soc.,* **84**, 195-201.

____, K. Gilbert, R. Cosgrove, D. P. Ruth, and K. Sheets, 2009: The gridding of MOS. *Wea. Forecasting*, **24**, 520-529.

Iredell, M., and P. Caplan, 1997: Four-times-daily runs of the AVN model. NWS Technical Procedures Bulletin No. 442, National Oceanic and Atmospheric Administration, U.S. Department of Commerce, 3 pp.

NWS, 2007: *NWS Focus*. National Weather Service, National Oceanic and Atmospheric Administration, U.S. Department of Commerce, 19 pp.

Schaefer, T. J., 1990: The critical success index as an indicator of warning skill. *Wea. Forecasting*, **5**, 570-575.